SWASH FLOWS GENERATED BY A TRAIN OF SOLITARY WAVES ON A PLANAR SLOPE

In Mei Sou, National University of Singapore, inmeisou@gmail.com
Yun-Ta Wu, National Cheng Kung University, ytwu@gs.ncku.edu.tw
Philip L.-F. Liu, National University of Singapore, philiplfliu@gmail.com

INTRODUCTION

The objective of this study is to gain insights of the swash flows generated by a train of solitary waves on a planar beach and the corresponding turbulence structure. Two-dimensional velocity measurements are made using a 1000-Hz high speed particle image velocimetry (HSPIV). The turbulence characteristics in terms of the temporal and spatial evolution of the turbulent kinetic energy (TKE), TKE spatial spectra, and turbulence length scales are examined.

WAVE CONDITIONS

A 5-m long-stroke wavemaker is used to generate six consecutive solitary waves, propagating over an 1/10 slope. The time separation between two consecutive waves is roughly the characteristic wave period. Following the solitary wave breaking criterion (Grilli et al. 1997), two wave conditions are examined: (1) a leading non-breaking (NB) solitary wave with subsequent surging breakers and (2) a leading surging-breaking (SB) solitary wave with subsequent plunging breakers. These two cases are a weakly interacting case (NB) and a strongly interacting case (SB), respectively (Wu et al. 2021).

RESULTS

Swash flow reaches the quasi-steady state after the third solitary wave for both NB and SB cases. For the NB case, non-stationary hydraulic jump occurs during the interaction between the downwash and uprush flows. The hydraulic jump evolves into a broken bore with the counterclockwise motion due to the bed-generated eddies during the downwash phase. Contrarily, the separation time between two waves for the SB case is too short for the hydraulic jump to happen. The second solitary wave arrives before the downwash flow depth of the first wave completely disappears, while the downwash flow is still strong. The plunging breaker generates an uprush broken bore with clockwise rotation inside the front roller fluid domain and counterclockwise eddies along the bed.

Using the TKE spatial spectra during the uprush and downwash flows, the turbulence structures at the quasi-steady state are compared between the NB and SB cases. Each spectrum is calculated using the spatial data in the x-direction at an elevation z and is normalized with the variance of the turbulent velocity $\langle u^2 \rangle$ and $\langle w^2 \rangle$, respectively. The time instant t is normalized with the wave period T and the phase $t/T = 0$ is defined as the instant of the flow reversal from the downwash to the uprush phase. Figure 1 shows the horizontal spectrum $\langle S_{uu} \rangle$ and the vertical spectrum $\langle S_{ww} \rangle$ during the downwash phase at $t/T = -0.114$ for the NB and SB cases. The TKE level in the vertical spectrum $\langle S_{ww} \rangle$ is lower as compared to the horizontal spectrum $\langle S_{uu} \rangle$ in both cases, suggesting that the boundary effect is important near the bed. The TKE energy level during the downwash phase for the NB case is higher than the SB case due to the non-stationary hydraulic jump during the downwash for the NB case. The energy injection at the wavenumber $\kappa_1 \approx 300$ rad/m shown in spatial turbulent energy spectra is of the order of the integral length scale. The SB case behaves similarly to the unsteady boundary layer flow during the downwash phase with a "-1 slope" in the energy cascade because of the energy injection from the larger eddies with the length scale of the order of the integral length scale.

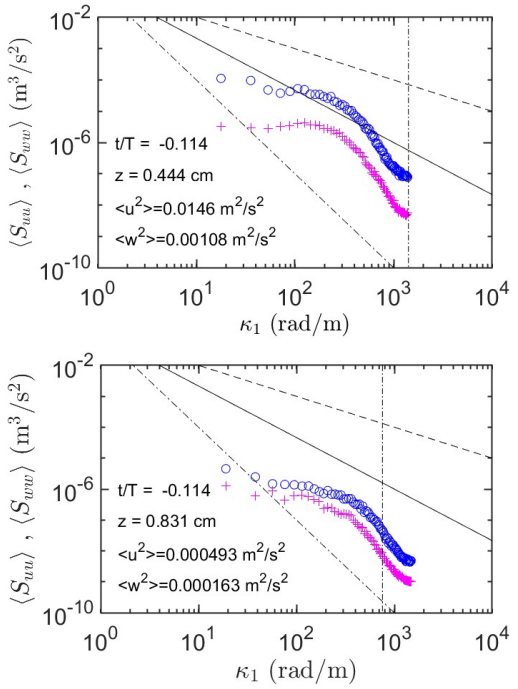

Figure 1 - Spatial turbulent kinetic energy spectra during the downwash phase for the NB case (top) and the SB case (bottom): $\langle S_{uu} \rangle$ (o); $\langle S_{ww} \rangle$ (+); -5/3 slope (——); 1 slope (-----); -3 slope (- · - · -)

Figure 2 shows the TKE spectra during the uprush phase at for the NB and SB cases. The TKE energy level for both cases are roughly at the same order of magnitude because of the broken bore during the uprush for both cases.

The time-dependent integral length scale represents the correlation distance of turbulent velocity in space and the largest eddy size in the flow. The integral length scale is evaluated directly using the one-dimensional spatial

spectrum (Pope 2000) as

$$\langle L_{xx}\rangle_{\kappa_1} = \frac{\pi}{2}\frac{\langle S_{uu}(k_1=0)\rangle}{\langle u^2\rangle}, \quad \langle L_{zz}\rangle_{\kappa_1} = \frac{\pi}{2}\frac{\langle S_{ww}(k_1=0)\rangle}{\langle w^2\rangle}. \qquad (1)$$

Since the wavenumber in the x-direction $\kappa_1 = 0$ cannot be resolved with the spatial data, the spectrum energy level at the smallest κ_1 is used to calculate the integral length scale.

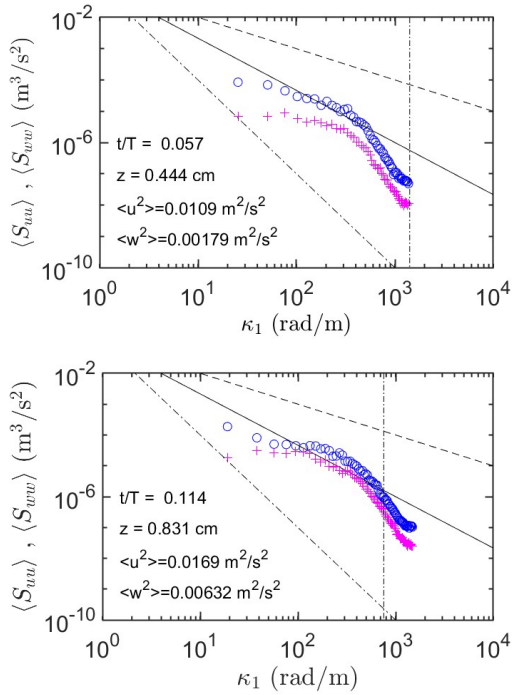

Figure 2 - Spatial turbulent kinetic energy spectra during the uprush phase for the NB case (top) and the SB case (bottom): $\langle S_{uu}\rangle$ (o); $\langle S_{ww}\rangle$ (+); -5/3 slope (——); 1 slope (-----); -3 slope (-·-·-·-)

Figure 3 shows the evolution of the vertical variation of the integral length scales. During the downwash flow the integral length scale is larger near the bed and smaller as the elevation increases for the NB45 case (Figure 3, left column from $t/T = -0.114$ to 0.114). This is because the eddies generated from the bed eventually diffused into the upper water column. For the SB case, that the integral length scale can be as large as the local water depth during the downwash phase (Figure 3, right column at $t/T = -0.114$). The integral length scale is larger near the bed and smaller in the water column due to the influence from the next incoming breaking wave (Figure 3, right column at $t/T = 0.000$). The magnitude of the integral length scale is roughly between 1 cm to 2 cm, which is the same order of magnitude as shown in the energy injection in the spatial spectra at $\kappa_1 =$ 200 rad/m to 300 rad/m (Figure 1 and 2).

Figure 4 shows an example of the HSPIV raw image during the downwash flow. The bed-generated eddies with the length scale of the order of the integral length scale are revealed by the seeding particles.

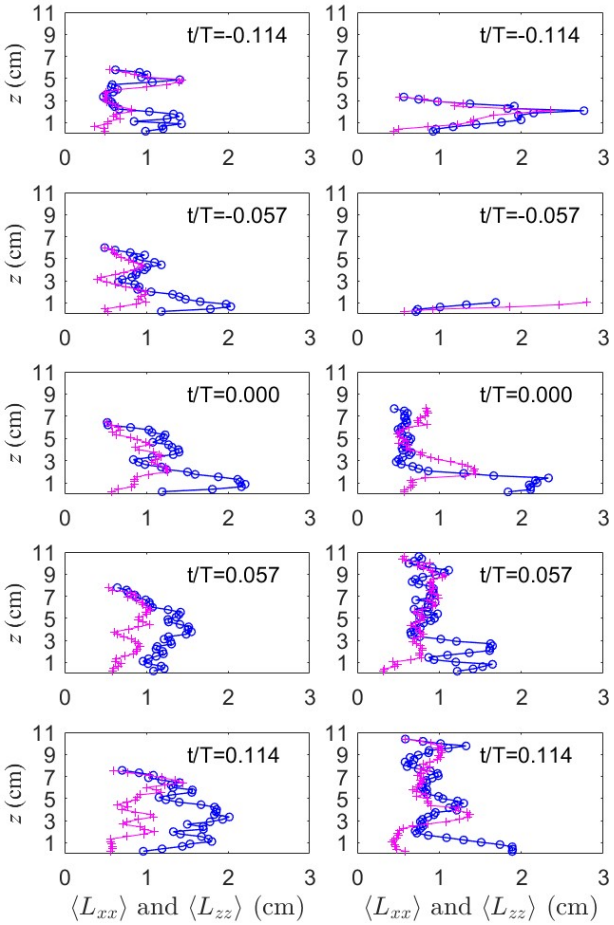

Figure 3 - Spatial variation of the integral length scales at various time for the NB case (left column) and the SB case (right column): $\langle L_{xx}\rangle$ (o); $\langle L_{zz}\rangle$ (+)

Figure 4 - Example of bed-generated eddies during the downwash revealed by the seeding particles in the HSPIV raw image

REFERENCES

Grilli, Svendsen, Subramanya (1997): Breaking criterion and characteristics for solitary waves on slopes, Journal of waterway, Port, Coastal, and Ocean Engineering, vol. 113, pp. 102-112.

Pope (2000): Turbulent Flows. Cambridge University Press.

Wu, Higuera, Liu (2021): On the evolution and runup of a train of solitary waves on a uniform beach, Coastal Engineering, vol. 170, 104015.